Published in final edited form as:
J Am Chem Soc. 2010 April 28; 132(16): 5803–5811. doi:10.1021/ja100598e.

Changes in Transmembrane Helix Alignment by Arginine Residues revealed by Solid-State NMR Experiments and Coarse-Grained MD Simulations

Vitaly V. Vostrikov[1,#], **Benjamin A. Hall**[2,#], **Denise V. Greathouse**[1], **Roger E. Koeppe II**[1,*], and **Mark S. P. Sansom**[2,*]

[1]Department of Chemistry and Biochemistry, University of Arkansas, Fayetteville, Arkansas 72701, USA

[2]Department of Biochemistry & Oxford Centre for Integrative Systems Biology, University of Oxford, South Parks Road, Oxford, OX1 3QU, UK

Abstract

Independent experimental and computational approaches show agreement concerning arginine/membrane interactions when a single arginine is introduced at selected positions within the membrane-spanning region of acetyl-GGALW^{5}LALALAL^{12}AL^{14}ALALW^{19}LAGA-ethanolamide, designated GWALP23. Peptide sequence isomers having Arg in position 12 or position 14 display markedly different behaviors, as deduced by both solid-state NMR experiments and coarse-grained molecular dynamics (CG-MD) simulations. With respect to the membrane normal of DOPC or DPPC lipid bilayer membranes, GWALP23-R14 shows one major state whose apparent average tilt is ~10° greater than that of GWALP23. The presence of R14 furthermore induces bilayer thinning and peptide displacement to "lift" the charged guanidinium toward the bilayer surface. By contrast, GWALP23-R12 exhibits multiple states that are in slow exchange on the NMR time scale, with CG-MD simulations indicating two distinct positions with different screw rotation angles in the membrane, along with an increased tendency to exit the lipid bilayer.

Keywords

lipid bilayer; WALP peptide; tryptophan; arginine; deuterium magnetic resonance; coarse-grained molecular dynamics simulation

Membrane proteins play a major role in a range of biological processes, as they represent about 25% of encoded gene products1 and ~40% of drug targets.2 The structure and function of membrane proteins may be modulated by interactions with their lipid bilayer environment.3 The understanding of how membrane proteins interact with lipid bilayers4 has been aided by studies of "simple" model transmembrane (TM)5 α-helices such as the WALP series of

*Roger E. Koeppe II, 119 Chemistry Building, University of Arkansas, Fayetteville, AR 72701, USA. Phone: 479-575-4976. Fax: 479-575-4049. rk2@uark.edu. *Mark S. P. Sansom, Department of Biochemistry, University of Oxford, South Parks Road, Oxford, OX1 3QU, United Kingdom. Phone: +44 1865 613306. Fax: +44 1865 613238. mark.sansom@bioch.ox.ac.uk.
#These authors made equal contributions to the work.

Supporting Information available
Circular dichroism spectra for GWALP23, GWALP23-R12 and GWALP23-R14 in DOPC. Deuterium NMR spectra of peptides with a single Ala-d$_4$ label in the sequence. Natural abundance deuterium NMR spectra of DOPC lipids. GALA fits for GWALP23 and GWALP23-R14 with different order parameter values. Tilt-rotation plots derived from CG-MD. Physical data for GWALP23-R12 (HPLC, mass spectrum). This material is available free of charge via the Internet at http://pubs.acs.org.

peptides. These peptides consist of a variable length poly-alanine/leucine core capped at either end with tryptophan residues that favor the membrane/water interface.6–13 WALP peptides have been employed to study a wide range of transmembrane helix behaviors, including hydrophobic mismatch, variation of helix tilt with varying peptide and lipid lengths, and helix dimerization, amongst others. Recently, a novel related peptide was described, GWALP23 (acetyl-GGALW$(LA)_6$LWLAGA-ethanolamide),[14] which differs from the WALP family in having only a single tryptophan residue near each terminus. The defined orientation and dynamics[14] of GWALP23 provide exceptional opportunities for investigating the influence of guest residues such as arginine upon the properties and lipid interactions of membrane-spanning peptide helices.

The role and behavior of arginine residues in membrane proteins is the subject of ongoing debate. Arginine residues in TM helices have an important biological role in the voltage sensor domains of voltage activated channels and enzymes[15] and have been especially studied in the context of voltage-dependent potassium channels[16–19] and cell-penetrating peptides.[20,21] Due to its high pK_a, the arginine side chain retains a positive charge over a wide range of pH and dielectric constant environments. The interactions of arginine with lipid bilayers have gained considerable attention, within a context that interactions with the membrane interior are quite different from those at the membrane/solution interface.[22–26]

In this article we present experimental and computational approaches to probe the arginine interaction with lipid bilayer membranes by employing GWALP23 and derivatives. Substitution of leucine (L) with arginine (R) at position 14 or 12 (L14R or L12R) results in peptides having one single Arg placed close to the center of the membrane-spanning segment of GWALP23 (Figure 1). Since the radial separation between the Trp side chains is small, an Arg can be positioned so that it will project either from the same side as both Trp indole rings (R12), or from a different face of the helix (R14). Figure 1 depicts both atomic and coarse-grained (CG) representations of the Arg and Trp side chains projecting from the GWALP23 helical backbone.

To understand the influence of R14 and R12 upon lipid bilayer membrane-incorporated GWALP23, solid-state NMR experiments and molecular dynamics (MD) simulations were undertaken. Circular dichroism spectra will show that the peptides remain helical in the lipid environments. The introduction of ^{2}H-labeled alanines into the helical sequences enables the helix orientations with respect to the DOPC bilayer membrane normal to be assessed using the "Geometric Analysis of Labeled Alanines" (GALA) method.[7] In parallel, the application of coarse-grained molecular dynamics (CG-MD) simulations27–29 allowed us to assess the behavior of these peptides in DPPC or DOPC lipid bilayers. CG-MD overcomes the typical time-scale limitations of atomistically detailed simulations of membrane proteins30 by combining ~4 non-hydrogen atoms to form a single CG particle. The experiments and simulations give fundamental agreement, with both methods showing markedly different behavior between the R12 and R14 derivatives of GWALP23.

Results

NMR spectra of bilayer-incorporated peptides

The ^{2}H NMR spectra of labeled alanines (Figure 2) reveal obvious differences between bilayer-incorporated samples of the GWALP23-R12 and -R14 peptide sequence isomers. GWALP23-R14 exhibits distinct pairs of signals for the CD_3 methyl side chains of all six core alanines, with spectral quality comparable to that of native GWALP23.[14] The pattern of ^{2}H quadrupolar splittings suggests dynamic averaging about a single predominant state, which is a tilted transmembrane (TM) helix for GWALP23-R14. Conversely, spectra of the R12 variant are characterized by poor signal-to-noise ratio, even though twice as many free induction decays

were collected. Multiple low-intensity broad peaks are observed for each labeled Ala in GWALP23-R12, suggesting two or more states for this peptide, in slow exchange with respect to the lipid bilayer membrane. Tabulated quadrupolar splittings ($\Delta\nu_q$) for the core ^{2}H-alanines in GWALP23-R12 and -R14 are provided in Table 1.

Given the differences in the ^{2}H NMR spectra it is important to consider whether the GWALP derivatives remain helical. Indeed, circular dichroism spectra (Figure S1 of the Supporting Information) indicate that GWALP23-R12 and GWALP23-R14 retain the primarily α-helical secondary structure observed for GWALP23 in DOPC. Although the far-UV region (<203 nm) is not accessible due to strong absorption by the DOPC double bond, the features of an α-helix (a minimum at 208 nm and a shoulder at 222 nm) are readily recognized in each of the spectra. The three peptides exhibit similar mean residue ellipticity values, with comparable $\varepsilon_{208}/\varepsilon_{222}$ ratios. It is significant that the GWALP23-R12 helix does not appreciably unwind when interacting with the DOPC bilayers.

To estimate the charged state of the Arg guanidinium side chain, selected samples were prepared using buffer at either pH 7.4 or pH 4.5, to maintain a constant microenvironment for the arginine. The buffer samples at both pH levels yield spectra of similar quality and identical $\Delta\nu_q$ values to the buffer-free samples prepared with ^{2}H-depleted water (Figure 3). Because the R14 and R12 side chains undoubtedly both carry a positive charge at pH 4.5, the similar results at pH 7.4 and 4.5 indicate that the guanidinium groups remain charged in all of the samples and experiments reported here. Variations in peptide/lipid ratio from 1/40 to 1/80, or in temperature (30–50 °C), also yielded no significant spectral changes.

Individual signals in the spectra for GWALP23-R14 were assigned and then were analyzed using the GALA method, while incorporating a variable order parameter S_{zz} for the peptide and keeping the $\varepsilon_{//}$ angle fixed at 59.4°.[7,31,32] The best fit for the tilt of GWALP23-R14 (Table 2; Figure 4) occurs for a relatively high S_{zz} value of 0.94, compared to 0.86 for GWALP23 itself. Introduction of R14 caused the apparent average tilt of the GWALP23 helix axis to increase ~10° (relative to the DOPC bilayer normal). Furthermore the direction of the tilt, relative to the G1 reference point,[7] changed by ~75°. Despite the presence of Arg near the helix center, the peptide retains predominantly a TM orientation. (One is unable to resolve NMR signals representing minor populations.) The ^{2}H NMR spectra of GWALP23-R14, in addition to strong C_β-D_3 peaks, furthermore exhibit some weaker signals from backbone C_α-D (Figure 2). This observation is noteworthy, since C_α-D signals have been observed also when proline is introduced near the center of WALP19,[32] but otherwise not in WALP family peptides, including GWALP23.[11,14,33] The result could signify that the motional regime of GWALP23-R14 is different from other WALP family peptides that lack Arg or Pro. The $\Delta\nu_q$ values of both the GWALP23–R14 and – R12 alanines, recorded at β=90°, are half of the corresponding $\Delta\nu_q$ values recorded at β=0°, indicating that both peptides undergo rapid reorientation (faster than ~4×10^4 s^{-1}) about the DOPC bilayer normal.[34] The peptide tilt and this "precession" motion[35] together define a cone angle of about 17° for GWALP23-R14 in DOPC.

For the case of GWALP23-R12, multiple peaks are observed in samples with two Ala labels (Figure 2B), or even when only one Ala is labeled (Figure S2 of the Supporting Information). (Control experiments with DOPC alone show that the central pair of very sharp signals—also present in Figure 2A—is from the lipid background (Figure S3). The other peaks from GWALP23-R12 are notably broad and cannot be attributed to natural abundance deuterium in DOPC.) As noted above, CD spectra indicate that the helical secondary structure is largely maintained even with the L12R substitution (Figure S1). With the alanine CD_3 signals being broadened and showing reduced intensity, it is very unlikely that any backbone C_α-D signals for GWALP23-R12 could be observed in these spectra. We therefore attribute the multiple NMR signals to multiple states for the helical backbone that holds the Ala side chains. It is

remarkable that some quadrupolar splittings as large as 55 kHz are observed for GWALP23-R12 Ala methyls. For alanine CD_3 groups to exhibit such high $\Delta\nu_q$ values, the helix axis would be nearly perpendicular to the membrane normal, corresponding to an interfacial orientation of the peptide. Multiple signals from each labeled alanine (Figures 2–3; Table 1) imply that several distinct populations of GWALP23-R12 co-exist and exhibit slow exchange. (In principle, GWALP23-R14 also "could" have multiple populations, but they would have to be in fast exchange, since they yield one set of signals.) Together, the experimental data suggest that GWALP23-R12 is present in DOPC as an α-helical peptide which assumes several orientations, at least one of which is a surface bound (interfacially oriented) helix. While slower dynamic averaging is likely responsible not only for distinct populations but also for line broadening, still the dynamics within an individual state are not so slow as to eliminate the signal averaging that gives rise to the pairs of peaks when samples of GWALP23-R12 are oriented at β=90°.

CG-MD simulations

To gain further insight into the interactions of these peptides with lipid bilayers, we performed CG-MD simulations. In these simulations, a model helix and randomly positioned lipid (DPPC) molecules and waters were used to self assemble to form a helix/bilayer system. Previous applications of this simulation method (which uses a forcefield derived from the MARTINI[36] forcefield) for a number of membrane peptides29 and proteins37 have yielded good comparisons with experimental data. For each peptide an ensemble of 100 individual self-assembly simulations, each of duration 100 ns (Figure 5), was performed in order to provide adequate sampling of peptide/bilayer interactions. For each ensemble of simulations, the results were analyzed in terms of three key metrics describing the orientation relative to the lipid bilayer: (i) the displacement of the helix relative to the center of the bilayer; (ii) the tilt of the helix axis relative to the bilayer normal; and (iii) the screw rotation of the helix (about its long axis). The parent GWALP23 helix is seen to adopt a TM orientation (Figure 6), with a mean tilt angle of ~15° and its center of mass close to the center of the bilayer (i.e. displacement ~0 Å). The GWALP23-R14 peptide, in which the Arg side chain is on the opposite side of the α-helix from the two Trp side chains, also adopts mainly (82% of the time) a TM orientation. However, there is a clear increase in the tilt angle of GWALP23-R14 by ~10° relative to the parent GWALP23 helix, in good agreement with the NMR experiments. The GWALP23-R14 helix is also displaced by ~5 Å towards the leaflet adjacent to the C-terminus of the helix. Visualization of the simulations indicates furthermore that the R14 side chain snorkels to the interfacial region, adjacent to the C-terminus of the helix. The presence of GWALP23-R14 also creates a local thinning of the bilayer (by 2.5 Å) relative to unmodified GWALP23, as well as increasing contacts of the peptide with water and phosphate particles. There is also a change of ~70° in the screw rotation of the GWALP23-R14 helix relative to GWALP23, again in good agreement with NMR data, and a narrowing of the distribution of rotation angles observed. By calculating the absolute rotation angles we are able to confirm close agreement between the rotation angles of the peptides adopted in the CG-MD simulations and the GALA analyses (Table 2), confirming that the CG tryptophans are correctly oriented in the bilayer. There remains a small difference (~8°) between the absolute tilt values calculated from the different methods, but this may arise from differences in the algorithms used to calculate these angles in the experimental and simulation systems. In addition, the distributions of rotation and tilt angles closely resemble the distributions observed in contour plots of rotation and tilt from GALA analysis (Figures 4, S4 and S5). HELANAL analysis also reveals that as expected the secondary structure restraints in the coarse grain model prevent any significant difference in bending being observed between GWALP23 and GWALP23-R14, which would agree with CD data indicating that helicity is maintained.

The behavior of GWALP23-R12 in CG-MD simulations is quite different. The helix adopts three different orientations, two TM and one interfacial (labeled INT in Figure 6). In the TM orientations there are two different snorkeling regimes, in which the R12 side chain snorkels either N-terminally or C-terminally. Additionally, for a significant proportion of the simulation time (35%), the helix adopts an interfacial orientation (Figure 6). This frequency of the INT orientation is significantly higher than for either GWALP23 (~10%) or GWALP23-R14 (~20%). This is unlikely to arise from sampling effects within these simulations, as wider sets of data on the insertion of helical peptides in CG-MD demonstrate expected behaviors for artificial TM and interfacial peptides, and that these behaviors are not altered by extending the simulations (data not shown). Analysis of the screw rotation angle of the helix TM regime also demonstrates a bimodal distribution, occupying two distinct directions each ~50° away from the GWALP23 position. Visualisation of the simulations reveals quite clearly these three orientations of the GWALP23-R12 helix (Figure 7). The somewhat higher frequency of C terminal snorkeling may be explained by a higher energetic cost for moving the two glycines at the N terminus into the membrane core, as compared to the alanine/glycine residues at the C terminus.

The CG-MD simulations described above were repeated using a CG model of DOPC. The results (Figure 8) were similar in terms of tilt and rotation of the peptides, namely GWALP23-R12 exhibited a shift to an interfacial location. In terms of displacement, R14 again induced a smaller shift towards an interfacial orientation, yet only a single TM peak was seen. Thus, the observation of a shift from a TM orientation (GWALP23, GWALP23-R14) towards an interfacial location (GWALP23-R12) is robust with respect to changes in the lipid bilayer.

The CG models of the three orientations of GWALP23-R12 in a DPPC bilayer (at 323 K) were converted to atomistic (AT) models using a fragment based approach.[38] Each system was then simulated for 50 ns using AT-MD. In each case the peptide retained a largely α-helical conformation, and remained stably in its starting orientation. Thus, AT-MD simulations confirm that GWALP23-R12 may adopt multiple conformations relative to a phospholipid bilayer. Examinations of the atomistic GWALP23-R12 simulations also highlight the role for water penetration, as water molecules can be seen to enter the bilayer early in the simulation and then to remain in contact with the arginine side chain throughout the simulation (Figure 9). Examinations of the AT simulations reveal how water molecules and lipid phosphate groups interact closely with the arginine side chain.

Discussion

We have used a model TM helix (GWALP23) as the hydrophobic “host” for an arginine residue in order to unmask some of the complexities of the interactions of Arg-containing α-helices with lipid bilayers. This is a topic of relevance for the biosynthetic mechanisms and mode of action of voltage-sensor domains which are based upon an Arg-containing S4 helix.[15] Specifically, we have explored the effects on helix orientation within a bilayer of two particular arginine modifications of GWALP23 using both NMR and CG-MD to identify the distinct properties of the individual peptides. GWALP23-R14 is shown to undergo the same changes in helix tilt and rotation relative to GWALP23 in both simulation and experiment, indicating the likely accuracy of the simulation protocol and CG forcefield.36 The relatively small changes when R14 is introduced most likely reflect a competition of effects from tryptophan and arginine. In unmodified GWALP23, the tryptophans alone determine the helix orientation, with both Trp side chains lying close to the plane of the membrane interfacial region. The introduction of R14 alters the relative Trp positions by means of helix displacement. At the same time, side-chain snorkeling, in combination with helix displacement and tilt, will permit the R14 guanidinium to interact with the interfacial region, thereby allowing the helix to retain a TM orientation despite introduction of a positively charged side chain near the center of the

bilayer-spanning hydrophobic region. The combined helix displacement and side chain snorkeling can be viewed schematically as a positively-charged arginine "cork" making its way toward the bilayer interface (Figure 10).

To estimate the dynamics,[31,39] we have employed essentially "model 3" described by Strandberg *et al.*,[31] which incorporates a variable principal order parameter S_{zz} for the peptide. A value of 0.88 for S_{zz} gives a good fit for both GWALP23 and GWALP23-R14, with rmsd values between 0.6 and 1.0 kHz for both peptides (Table 2). If lower values of S_{zz} are tried, the apparent tilt τ increases slightly (Figure S4), the direction of tilt ρ does not change, and the rmsd increases, indicating poorer fits. While S_{zz} of 0.86 is "best" for GWALP23, the rmsd for GWALP23-R14 falls slightly (to 0.9 kHz) if S_{zz} is increased still more to 0.94. The GALA method, with dynamics, indicates $\Delta\tau$ of about 10° and $\Delta\rho$ of about −75° when R14 is introduced into GWALP23 (Figure 4; Table 2). Additionally, the independent ^{15}N PISEMA and ^{2}H GALA algorithms, with the latter incorporating S_{zz}, have shown good agreement concerning the tilt of GWALP23.[14] The further specific agreement here between NMR and CG-MD methods, concerning the changes in tilt as well as rotation between GWALP23 and GWALP23-R14, despite the small difference in the absolute tilt values (Table 2), highlights in this case a convergence of independent computational and experimental methods.

It is important to consider the possible limitations of the CG model used, which employs the MARTINI[36] parameters for lipids and peptides. As has been noted40 CG models such as MARTINI do not fully reproduce the thermodynamics of Arg insertion. Nevertheless, detailed comparison using a MARTINI-derived CG model41 suggested just a ca. 2-fold underestimation of the free energy barrier for burying a single Arg side chain in the bilayer core. Furthermore, comparisons of CG18 and atomistic[17] simulations of the S4 helix from Kv channels (which contains multiple Arg side chains) suggest that CG simulations are capable of (qualitatively) reproducing the local bilayer distortions caused by Arg insertion into a bilayer.

Furthermore, CG simulations of the Trp-containing WALP peptide helix29,36,[41] suggest that such CG simulations are capable of correctly capturing the interaction of Trp side chains with lipid bilayers. We also are reasonably confident that the observed difference between the R12 and R14 peptides is not simply a kinetic effect, as comparison with a wide range of TM and interfacial membrane peptides (Hall and Sansom, ms. in preparation) indicates that there exists sufficiently good sampling in the current studies to capture such a difference.

The combined results from the NMR and simulations reveal the subtle interplay of Trp and Arg side chains in orienting an α-helix relative to a lipid bilayer.[4] Thus the two tryptophan residues of GWALP23 and GWALP23-R14 determine the tilt of the helix relative to the bilayer normal; R14 dictates the rotational preference of the helix due to its tighter interaction with the interfacial region. The R14 snorkeling causes some bilayer deformation as observed in the CG-MD simulations, such that the bilayer is ~2.5 Å thinner in the presence of GWALP23-R14. This distortion is accompanied by water particles penetrating into the bilayer, as has been observed also in atomistic simulations.[17,19,24,25,42] It should be noted that the arginine side chain is indicated by the NMR experiments to be protonated (Figure 3), as has been suggested also by a number of calculations.[24,25]

It is encouraging that the relatively small difference in behavior of GWALP23-R14 relative to unmodified GWALP23 is highly consistent between NMR data and CG-MD simulations. The results suggest that the two methods are capable of reporting correctly on the effects of Arg residues on membrane/helix interactions. In GWALP23-R14 there seems to be cooperation between Trp and Arg to enable maximal access to the headgroup region; furthermore it is likely that W5 and W19 prevent further tilt by anchoring the peptide tips to the headgroup regions.

The behavior of GWALP23-R12 is strikingly different, arising from competition between the tryptophan and arginine side chains for access to the same lipid/water interfacial region. This dynamic competition leads to three different states being significantly populated: two TM orientations and one interfacial orientation. Thus, whether or not an arginine side chain may be accommodated within a hydrophobic TM helix is seen to depend on the sequence context in a non-linear fashion, which in turn reflects a competition for lipid headgroup and water interactions between the basic and the amphipathic aromatic side chains.

That the GWALP-R12 helix may adopt (meta-stable) TM state(s) in addition to an interfacial state is of interest as it may indicate a potential role for such multi-state behavior in biological as well as synthetic systems, providing thereby a potential orientational "switch" which could respond to changes in the helix/bilayer environment. Such changes may reflect the action of voltage-gated channels and cell-penetrating peptides, amongst others.

In summary, our combined experimental and computational approaches reveal that the introduction of a single arginine residue into a hydrophobic TM helix may result in either (i) a small reorientation of the helix relative to the bilayer interface (R14), or (ii) a dynamic switching between TM and interfacial orientations of the helix (R12). The identification of the charge status of arginine in the membrane through the use of different solution pH values clearly favors models in which the protonated form of the arginine side chain may insert into the membrane by inducing deformation of the bilayer. Further studies may reveal more details, including the role of adjacent TM helices in modulating such behavior in biological membranes.[26]

Materials and Methods

Experimental

Protected amino acids and "Rink" amide resin were purchased from NovaBiochem (San Diego, CA). Commercial L-alanine-d_4 from Cambridge Isotope Laboratories (Andover, MA) was modified with an Fmoc group, as described previously[32] and recrystallized from ethyl acetate:hexane, 80:20. Solid-phase peptide synthesis was performed on 0.1 mmol scale using a Perkin-Elmer / Applied Biosystems 433A synthesizer (Foster City, CA). Two Ala-d_4 residues were incorporated per peptide, at different isotope abundance levels, achieved by mixing appropriate amounts of Fmoc-L-Ala and Fmoc-L-Ala-d_4. Peptides were cleaved from resins using trifluoroacetic acid, resulting in amidated C-termini. Solvents were of the highest available purity. Peptides were purified by reversed-phase HPLC on an octyl-silica column using a gradient of 92–96% methanol, with 0.1% trifluoroacetic acid, over 24 min. Analytical HPLC results and MALDI-TOF analysis are provided in Figure S6 of the Supporting Information.

Mechanically aligned samples for solid-state NMR spectroscopy (1/60, peptide/lipid) were prepared using DOPC (Avanti Polar Lipids, Alabaster, AL) and deuterium-depleted water (Cambridge; 45% w/w hydration), as described previously.7 Deuterium NMR spectra were recorded on a Bruker Avance 300 spectrometer, utilizing a quadrupolar echo pulse sequence43 with 90 ms recycle delay, 3.2 μs pulse length and 115 μs echo delay. Between 750,000 (GWALP23-R14) and 1,500,000 (GWALP23-R12) transients were accumulated. An exponential weighting function with 100 Hz line broadening was applied prior to Fourier transformation. An enhanced GALA analysis7 was performed, using essentially model 3 of Strandberg *et al.*[31] to estimate the dynamics. This model employs a variable order parameter S_{zz} which can be divided (conceptually) into components S^i and S^r.[31] We utilized the helix and alanine geometry described previously and implemented an interactive grid search programmed in Microsoft Excel.[7,32]

Computational

Coarse-grained molecular dynamics (CG-MD) simulations of the peptides in ~128 lipid DPPC bilayer were performed. CG-MD overcomes the typical limitations of atomistically detailed simulations of biomolecules by combining ~ 4 non-hydrogen atoms to form a single CG particle. In the current study we have used the latest version of the MARTINI forcefield with protein parameters,36·44 running simulations using Gromacs v345 on a 56-processor Mac OS X cluster. Long range electrostatics were treated using a cut-off value of 12 Å and $\varepsilon = 20$ (additionally, results are robust at $\varepsilon = 15$). Temperature and pressure were coupled at 323 K and 1 Bar using the Berendsen46 weak coupling algorithm ($\tau_T = 1$ ps and $\tau_P = 10$ ps). The compressibility was 3×10^5 (1/bar). In each simulation the bilayer is allowed to self assemble around the peptide (Figure 5) to reduce potential sources of bias in the simulation. We have performed CG-MD simulations within a high throughput framework which enabled 100×0.1 μs simulations to be run (Hall & Sansom, manuscript in preparation) for each peptide helix, yielding good sampling of the helix/bilayer interactions.

Supplementary Material

Refer to Web version on PubMed Central for supplementary material.

Acknowledgments

This work was supported by grants from the US National Science Foundation (MCB-0841227), the Oxford Center for Integrative Systems Biology, the BBSRC and MRC, the Oxford Supercomputing Center, and the Arkansas Biosciences Institute. The NMR facility was supported by NIH grant RR 15569. Our thanks to Daniel Parton and Chze Ling Wee for useful discussions.

References

1. Wallin E, von Heijne G. Protein Sci 1998;7:1029–1038. [PubMed: 9568909]
2. Terstappen GC, Reggiani A. Trends Pharmacol. Sci 2001;22:23–26. [PubMed: 11165668]
3. Lee AG. Biochim. Biophys. Acta 2004;1666:62–87. [PubMed: 15519309]
4. Killian JA, von Heijne G. Trends Biochem. Sci 2000;25:429–434. [PubMed: 10973056]
5. **ABBREVIATIONS**, AT, atomistic; CD, circular dichroism; CG, coarse-grained; GALA, geometric analysis of labeled alanines; GWALP23, acetyl-GGALW$(LA)_6$LWLAGA-ethanolamide; MD, molecular dynamics; HPLC, high-performance liquid chromatography; MALDI-TOF, matrix-assisted laser desorption ionization time-of-flight mass spectrometry; TM, transmembrane.
6. de Planque MRR, Kruijtzer JAW, Liskamp RMJ, Marsh D, Greathouse DV, Koeppe RE 2nd, de Kruijff B, Killian JA. J. Biol. Chem 1999;274:20839–20846. [PubMed: 10409625]
7. van der Wel PCA, Strandberg E, Killian JA, Koeppe RE 2nd. Biophys. J 2002;83:1479–1488. [PubMed: 12202373]
8. de Planque MR, Bonev BB, Demmers JA, Greathouse DV, Koeppe RE 2nd, Separovic F, Watts A, Killian JA. Biochemistry 2003;42:5341–5348. [PubMed: 12731875]
9. de Planque MRR, Killian JA. Mol. Membr. Biol 2003;20:271–284. [PubMed: 14578043]
10. Killian JA. FEBS Lett 2003;555:134–138. [PubMed: 14630333]
11. Strandberg E, Özdirekcan S, Rijkers DTS, van der Wel PCA, Koeppe RE 2nd, Liskamp RMJ, Killian JA. Biophys. J 2004;86:3709–3721. [PubMed: 15189867]
12. Killian JA, Nyholm TKM. Curr. Opin. Struct. Biol 2006;16:473–479. [PubMed: 16828281]
13. Ozdirekcan S, Etchebest C, Killian JA, Fuchs PFJ. J. Am. Chem. Soc 2007;129:15174–15181. [PubMed: 18001020]
14. Vostrikov VV, Grant CV, Daily AE, Opella SJ, Koeppe RE 2nd. J. Am. Chem. Soc 2008;130:12584–12585. [PubMed: 18763771]
15. Swartz KJ. Nature 2008;456:891–897. [PubMed: 19092925]
16. Hessa T, White SH, von Heijne G. Science 2005;307:1427. [PubMed: 15681341]

17. Freites JA, Tobias DJ, von Heijne G, White SH. Proc. Natl. Acad. Sci. U. S. A 2005;102:15059–15064. [PubMed: 16217012]
18. Bond PJ, Sansom MSP. Proc. Natl. Acad. Sci. U. S. A 2007;104:2631–2636. [PubMed: 17301243]
19. Sands ZA, Sansom MSP. Structure 2007;15:235–244. [PubMed: 17292841]
20. Su Y, Doherty T, Waring AJ, Ruchala P, Hong M. Biochemistry 2009;48:4587–4595. [PubMed: 19364134]
21. Schmidt N, Mishra A, Lai GH, Wong GC. FEBS Lett. 2009 DOI 10.1016/j.febslet.2009.11.046.
22. Roux B. J. Gen. Physiol 2007;130:233–236. [PubMed: 17635960]
23. Dorairaj S, Allen TW. Proc. Natl. Acad. Sci. U. S. A 2007;104:4943–4948. [PubMed: 17360368]
24. Li L, Vorobyov I, MacKerell AD, Allen TW. Biophys. J 2008;94:L11–L13. [PubMed: 17981901]
25. MacCallum JL, Bennett WFD, Tieleman DP. Biophys. J 2008;94:3393–3404. [PubMed: 18212019]
26. Johansson ACV, Lindahl E. Proc. Natl. Acad. Sci. U. S. A 2009;106:15684–15689. [PubMed: 19805218]
27. Nielsen SO, Lopez CF, Srinivas G, Klein ML. J. Phys.: Condens. Matter 2004;16:R481–R512.
28. Marrink SJ, de Vries AH, Mark AE. J. Phys. Chem. B 2004;108:750–760.
29. Bond PJ, Holyoake J, Ivetac A, Khalid S, Sansom MSP. J. Struct. Biol 2007;157:593–605. [PubMed: 17116404]
30. Lindahl E, Sansom MS. Curr. Opin. Struct. Biol 2008;18:425–431. [PubMed: 18406600]
31. Strandberg E, Esteban-Martin S, Salgado J, Ulrich AS. Biophys. J 2009;96:3223–3232. [PubMed: 19383466]
32. Thomas R, Vostrikov VV, Greathouse DV, Koeppe RE 2nd. Biochemistry 2009;48:1183–1191. [PubMed: 19159235]
33. Ozdirekcan S, Rijkers DTS, Liskamp RMJ, Killian JA. Biochemistry 2005;44:1004–1012. [PubMed: 15654757]
34. Luo WB, Cady SD, Hong M. Biochemistry 2009;48:6361–6368. [PubMed: 19489611]
35. Lee J, Im W. Phys. Rev. Lett 2008;100:018103. [PubMed: 18232823]
36. Monticelli L, Kandasamy SK, Periole X, Larson RG, Tieleman DP, Marrink SJ. J. Chem. Theory Comput 2008;4:819–834.
37. Scott KA, Bond PJ, Ivetac A, Chetwynd AP, Khalid S, Sansom MSP. Structure 2008;16:621–630. [PubMed: 18400182]
38. Stansfeld PJ, Hopkinson RJ, Ashcroft FM, Sansom MSP. Biochemistry 2009;48:10926–10933. [PubMed: 19839652]
39. Esteban-Martin S, Salgado J. Biophys. J 2007;93:4278–4288. [PubMed: 17720729]
40. Vorobyov I, Li L, Allen TW. J. Phys. Chem. B 2008;112:9588–9602. [PubMed: 18636764]
41. Bond PJ, Wee CL, Sansom MS. Biochemistry 2008;47:11321–11331. [PubMed: 18831536]
42. Monticelli L, Robertson KM, MacCallum JL, Tieleman DP. FEBS Lett 2004;564:325–332. [PubMed: 15111117]
43. Davis JH, Jeffrey KR, Bloom M, Valic MI, Higgs TP. Chem. Phys. Lett 1976;42:390–394.
44. Marrink SJ, Risselada J, Yefimov S, Tieleman DP, de Vries AH. J. Phys. Chem. B 2007;111:7812–7824. [PubMed: 17569554]
45. Lindahl E, Hess B, van der Spoel D. J. Mol. Model 2001;7:306–317.
46. Berendsen HJC, Postma JPM, van Gunsteren WF, DiNola A, Haak JR. J. Chem. Phys 1984;81:3684–3690.

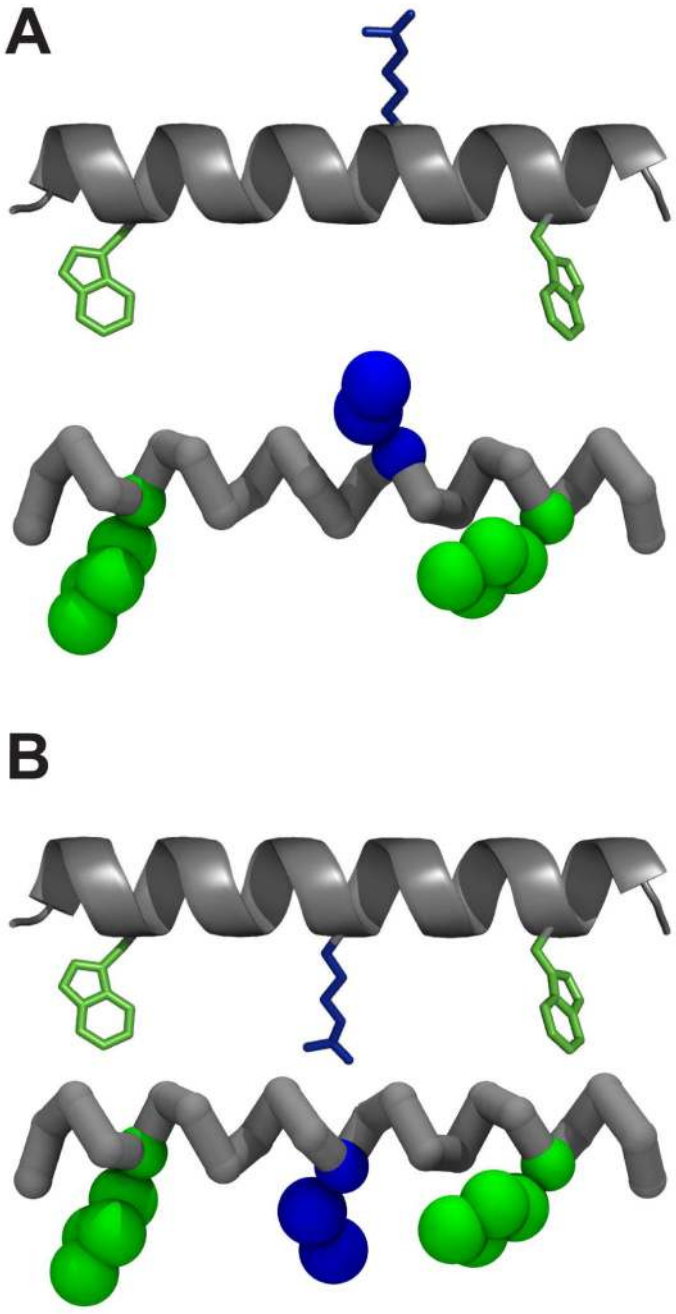

Figure 1.
Model structures of (A) GWALP23-R14 and (B) GWALP23-R12. In each case the atomistic side-chain model is shown on a ribbon helix above and the CG model below, with arginine (blue) and tryptophan (green) side chains. Note that the side chain of R14 is on the opposite side of the helix (A) from the tryptophan side chains, whilst the side chain of R12 is on the same side of the helix (B).

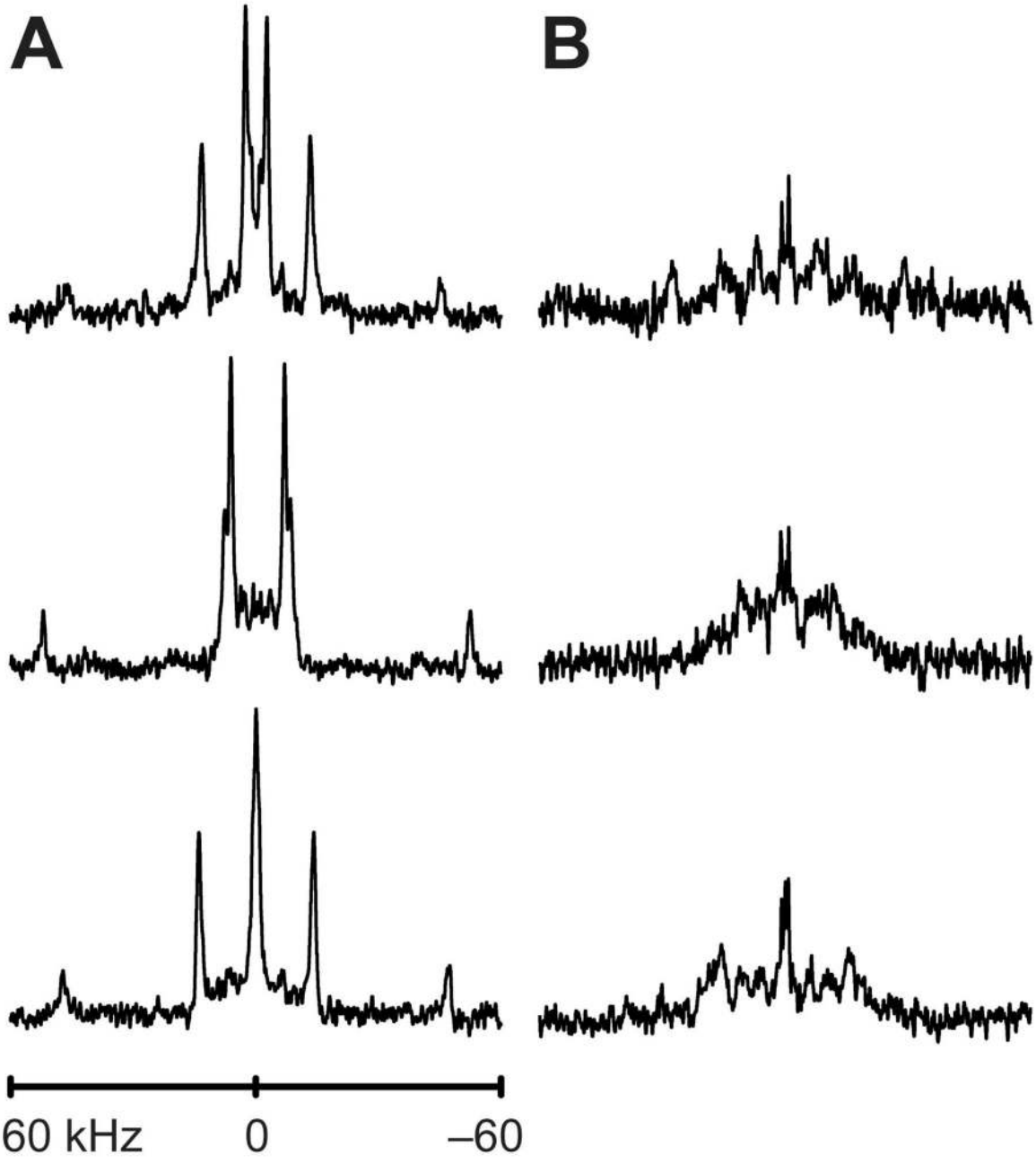

Figure 2.
Deuterium NMR spectra of (A) GWALP23-R14 and (B) GWALP23-R12 in hydrated, oriented bilayers of DOPC (peptide/lipid ratio 1/60; β=0° sample orientation; temperature 50 °C). The ^{2}H-labeled alanine residues are (top to bottom): 7 and 9; 11 and 13; 15 and 17.

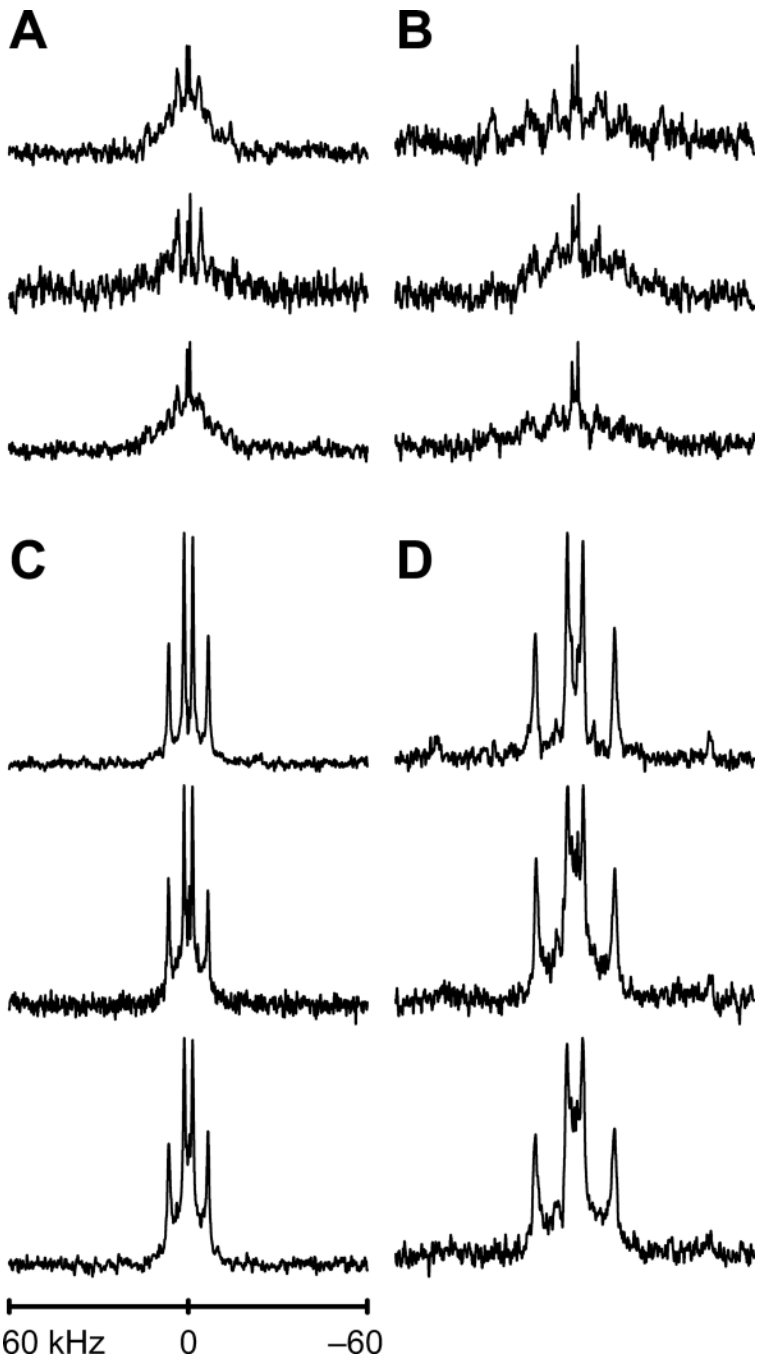

Figure 3.

Selected deuterium NMR spectra for two labeled alanines (7 and 9) in GWALP23-R12 (A, B) and GWALP23-R14 (C, D) in DOPC bilayers, hydrated with water, or with buffer at pH 7.4 or pH 4.5 (top to bottom), showing $\beta = 90°$ (A, C) and $\beta = 0°$ (B, D) sample orientations. Samples at pH 7.4 also contain 0.1 M NaCl. The peptide/lipid ratio is 1/60 at a temperature of 50 °C.

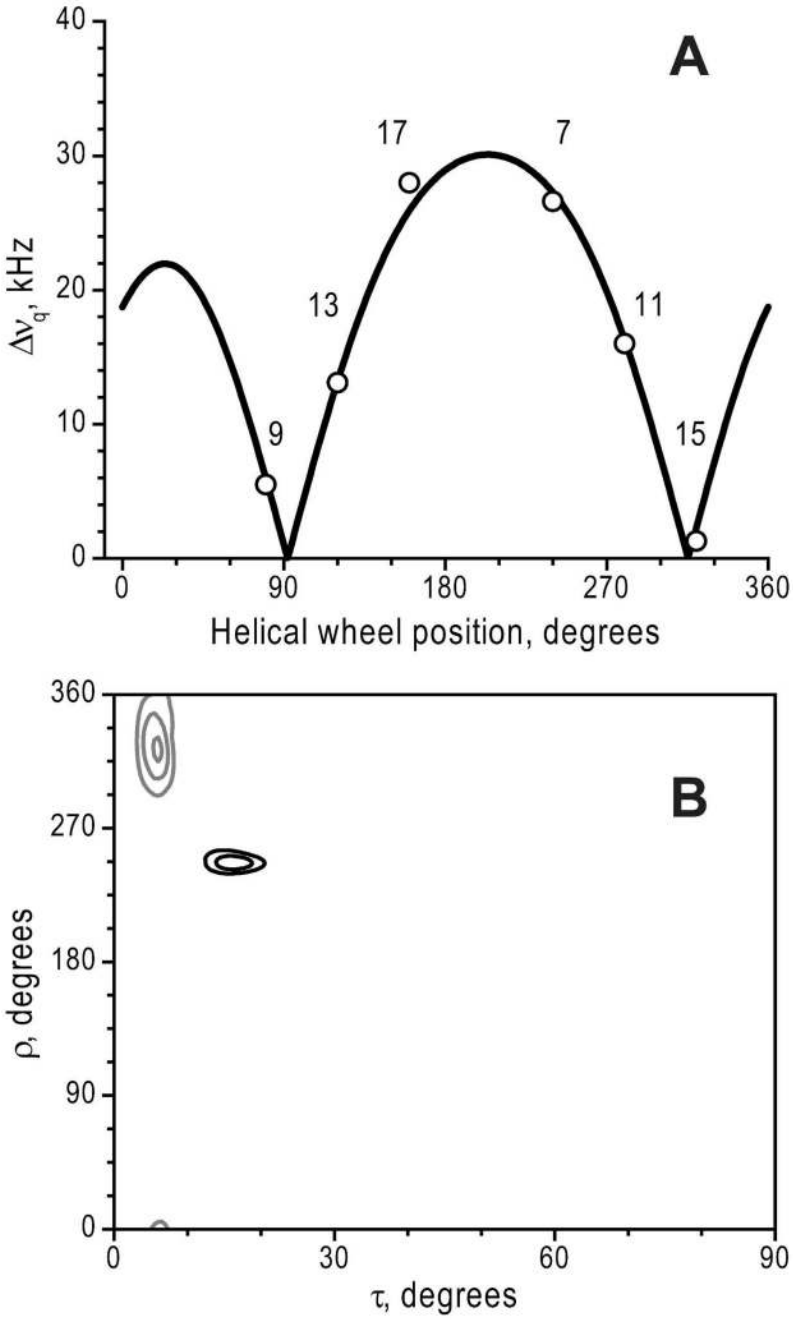

Figure 4.

GALA analysis of GWALP23-R14 average tilt in DOPC bilayer membranes, with variable S_{zz} and $\varepsilon_{//} = 59.4°$. (A) Quadrupolar wave plot with Ala positions indicated. (B) RMSD plot (contoured at 1, 2 and 3 kHz) for tilt τ and rotation ρ of peptides in DOPC: GWALP23 itself (gray); GWALP23-R14 (black). The global minima correspond to (S_{zz}, τ, ρ) of (0.86, 5.9°, 323°) and (0.94, 16.2°, 247°) respectively.

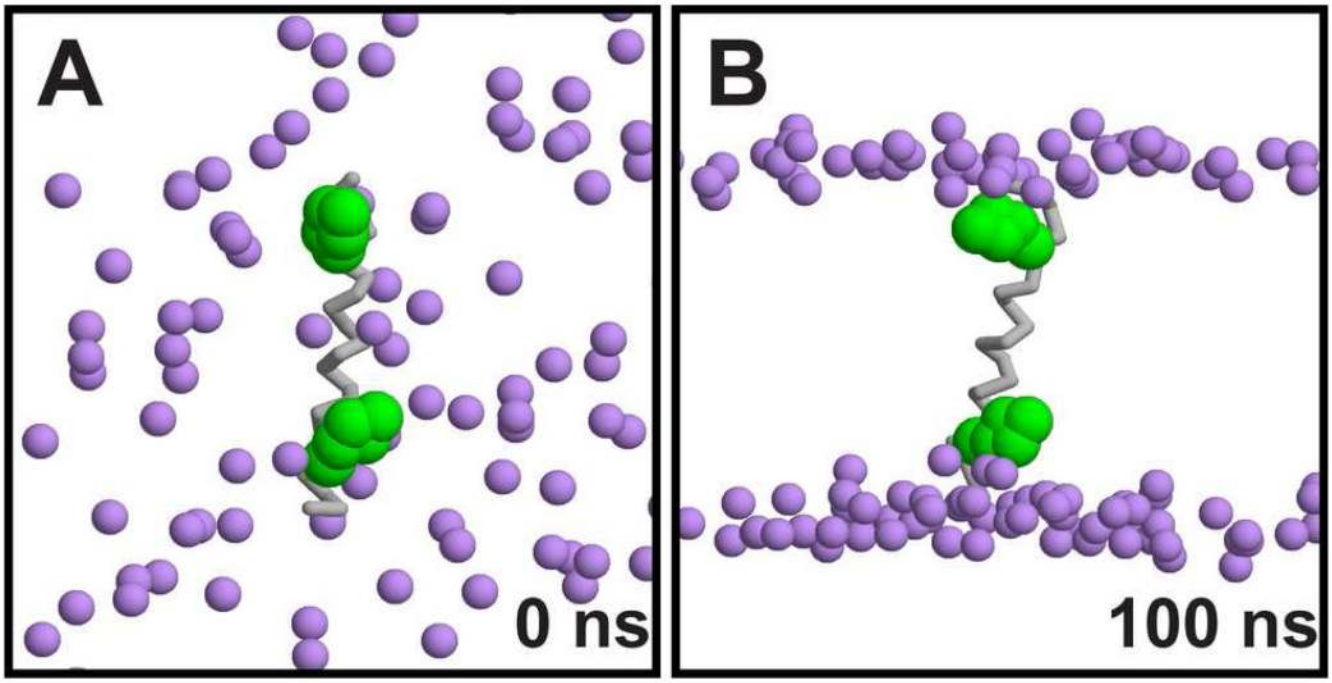

Figure 5.
Progress of CG simulation for GWALP23 in a DPPC bilayer. (A) Initial state (t = 0 ns) of the simulation system consisting of a GWALP23 α-helix (gray backbone, green Trp side chains) with randomly orientated phospholipids (purple spheres = phosphate particles) and waters (not shown). (B) Final state (t = 100 ns) of the system showing the GWALP helix tilted in a TM orientation with the Trp side chains close to the lipid headgroups.

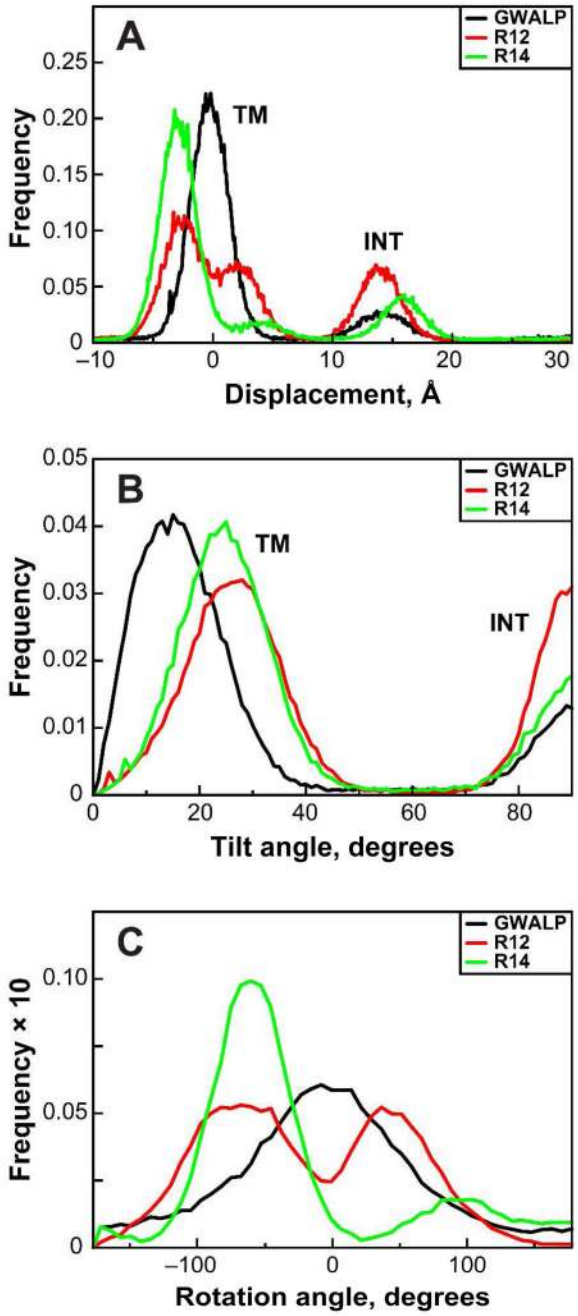

Figure 6.

Helix displacement relative to the DPPC bilayer center, tilt relative to the bilayer normal and rotation relative to that of GWALP23 in DPPC. Each curve is derived from analysis of an ensemble of 100 × 100 ns of CG simulations (analyzing the complete 100 ns simulations in each case). (A) Helix displacement, defined as the difference between the center of mass of the helix backbone and the center of the lipid bilayer. A displacement >10 Å is indicative of an interfacial (INT) orientation. Small negative displacements indicate moving a TM helix towards the C terminal facing leaflet; small positive displacements indicate moving a TM helix towards the N terminal facing leaflet. (B) Helix tilt, defined as the angle between the helix axis

and the bilayer normal. A tilt of 90° is indicative of an interfacial location. (C) Helix rotation, referenced to 0° as the tilt direction of GWALP23.

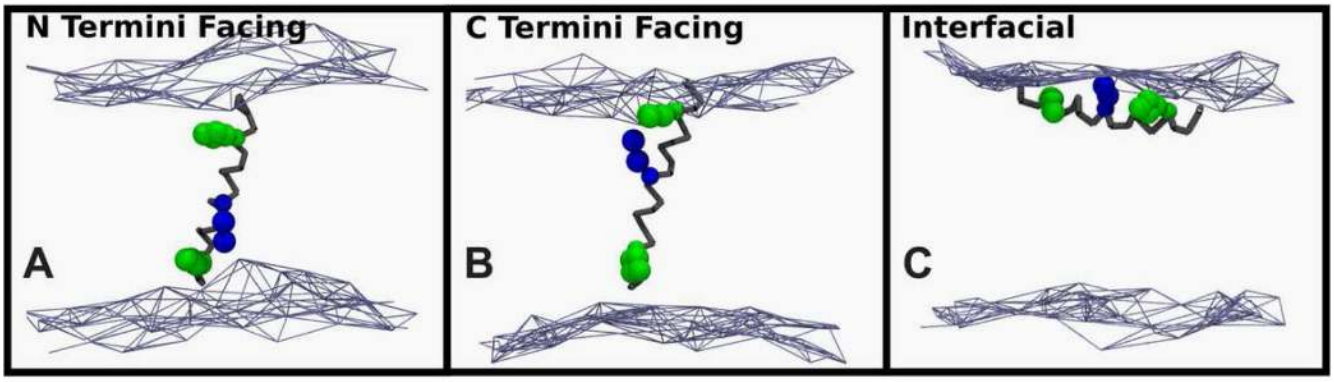

Figure 7.

Three orientations of the GWALP-R12 helix seen in CG simulations. The helix may adopt a TM orientation with the R12 side chain (blue) snorkeling towards either the N-terminal (A) or the C-terminal (B) face of the membrane. Alternatively, an interfacial orientation may be adopted (panel C). Trp side chains are green, Arg blue, and the bilayer surface (as defined by the phosphate particles) is a grey mesh.

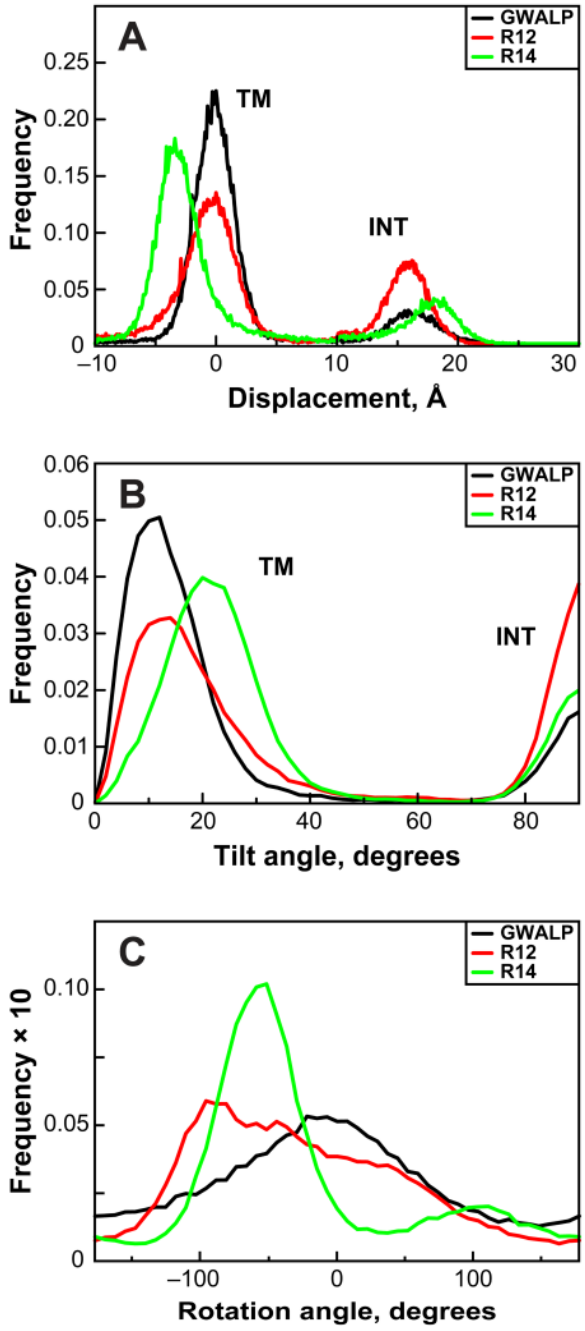

Figure 8.

Helix displacement and tilt in DOPC. Each curve is derived from analysis of an ensemble of 100 × 100 ns of CG simulations. (A) Helix displacement. (B) Helix tilt. (C) Helix rotation. The definition of terms is the same as in Figure 6.

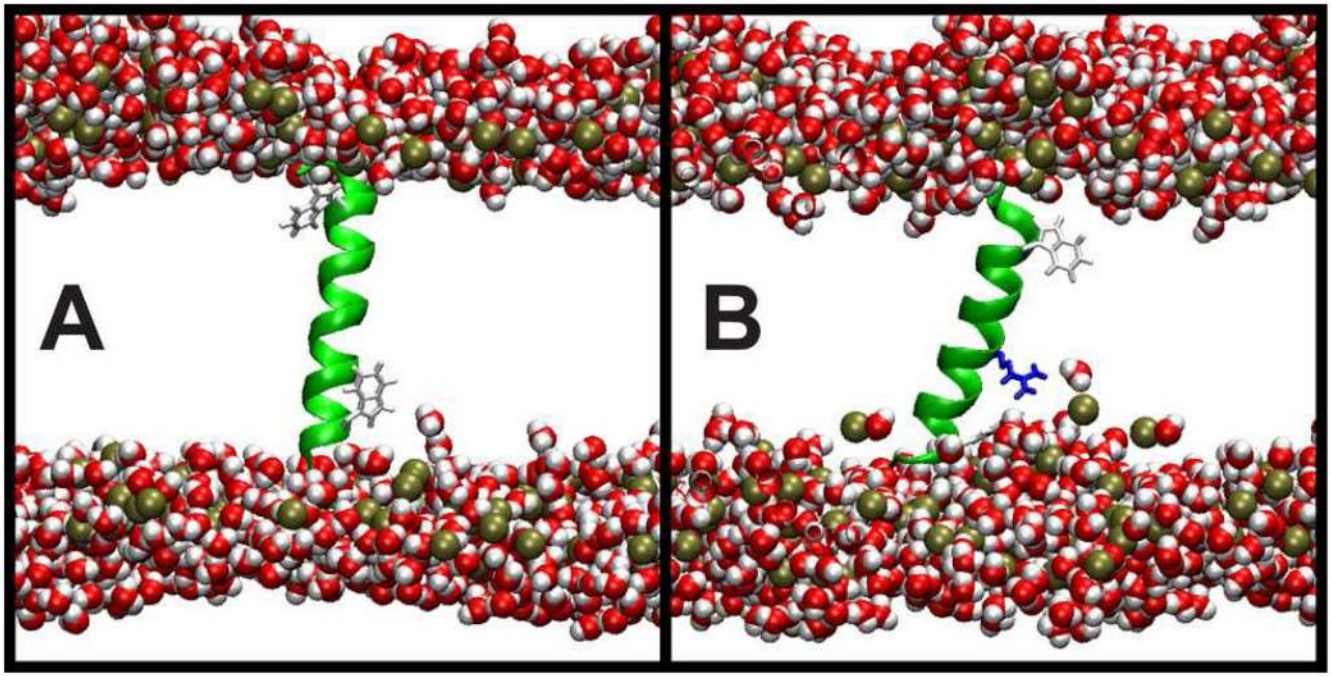

Figure 9.

Snapshots taken from atomistic simulations of (A) GWALP23 and (B) GWALP23-R12. Water and phosphate groups are in spacefill representations (red/white, and brown); the peptide backbone is shown with tryptophan and arginine residue side chains in stick representation. Bilayer deformation and water penetration can be clearly seen in the GWALP23-R12 simulation but not in the GWALP23 simulation, reflecting the effect of incorporating a charged arginine residue in the bilayer core.

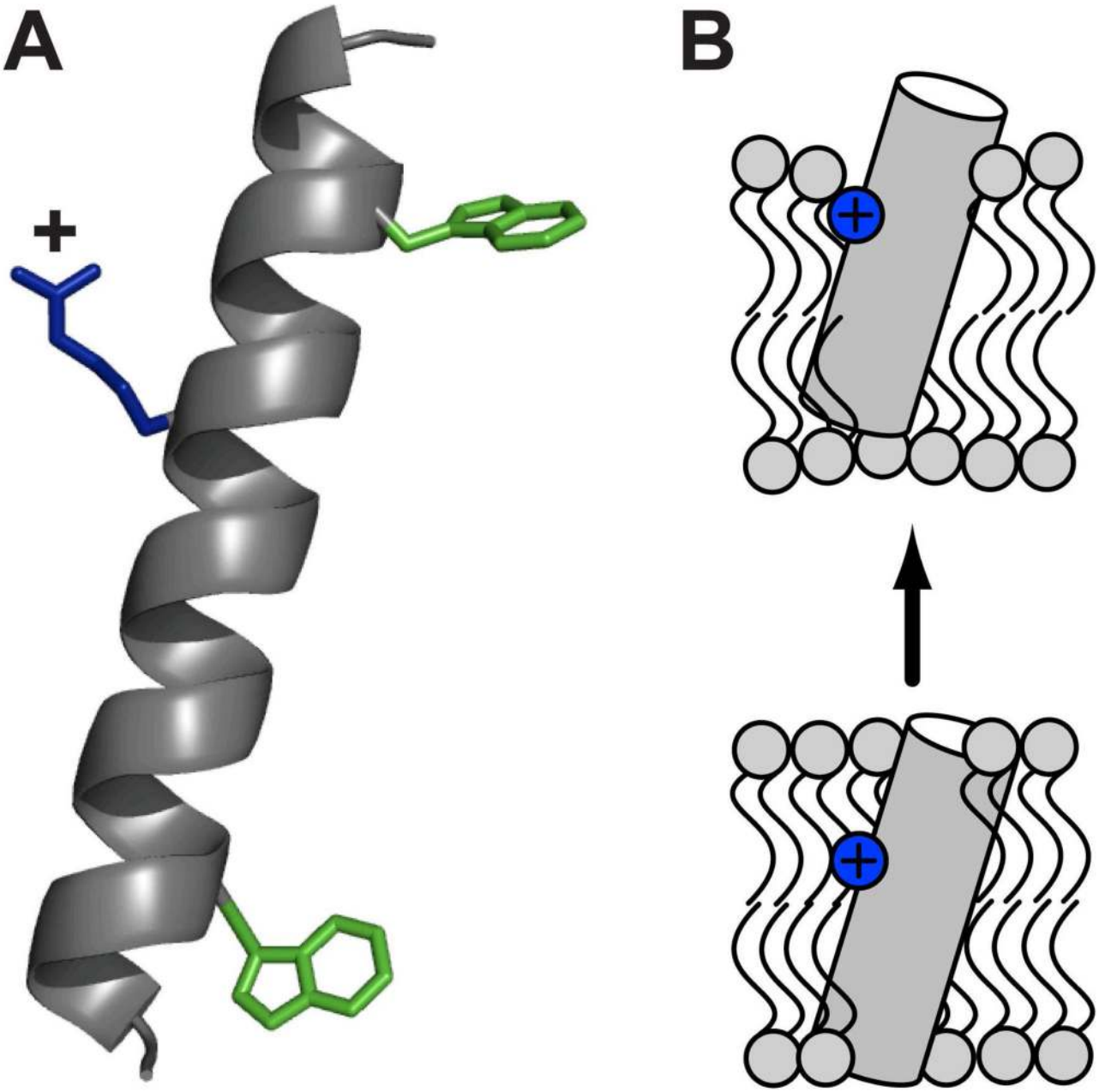

Figure 10.
(A) Model to illustrate the orientation of GWALP23-R14 tilted at ~17° with respect to the bilayer normal of DOPC. Side chains were constructed using a rotamer library and do not represent experimental data. (B) Schematic "cork" model for vertical displacement of GWALP23-R14 toward its C-terminal in a lipid bilayer membrane, as observed in the CG-MD simulations. Together the displacement and snorkeling, along with membrane thinning, allow the charged guanidium side chain to reach the bilayer-water interface.

Table 1

Quadrupolar splittings, $\Delta\nu_q$ in kHz, for ^{2}H-labeled core alanines of GWALP23-R14 and GWALP23-R12.[a]

Ala position	GWALP23-R14	GWALP23-R12[b]
5	26.6 kHz	3; 22; 32; 55
7	5.5	
9	16.0	2; 14; 22; 39
11	13.1	
13	1.3	2; 12; 21; 31
15	28.0	

[a] The quadrupolar splittings, $\Delta\nu_q$, are measured in kHz. The sample orientation is $\beta = 0°$ in hydrated DOPC bilayer membranes (peptide/lipid ratio 1/60; sample temperature 50 °C).

[b] Due to poor signal-to-noise, the values for GWALP23-R12 are approximate. Additionally, since multiple weak signals are observed for each double-labeled sample of GWALP23-R12, it is not possible to complete the individual assignments. Singly labeled samples of GWALP23-R12 (Figure S2 of the Supporting Information) also show multiple peaks; for these cases it still is not possible to correlate the assignments for the different alanines in the different peptide states.

Table 2

Comparison of average tilt and rotation angles of GWALP23 and GWALP23-R14 from GALA fits in DOPC and CG-MD simulations in DPPC and DOPC[a]

Peptide	Method	S_{zz}	rmsd[b]	τ	Δτ[c]	ρ	Δρ[c]
GWALP23	GALA	0.7	1.7	7.5°		318°	
GWALP23-R14	GALA	0.7	2.1	22.8°	15.3°	247°	−71°
GWALP23	GALA	0.8	0.8	6.5°		321°	
GWALP23-R14	GALA	0.8	1.4	18.6°	12.1°	247°	−74°
GWALP23	GALA	0.88	0.6	5.9°		323°	
GWALP23-R14	GALA	0.88	1.0	16.2°	10.3°	247°	−76°
GWALP23[d]	CG-MD /DPPC			15°		315°	
GWALP23-R14[d]	CG-MD /DPPC			25°	10°	245°	−70°
GWALP23[d]	CG-MD /DOPC			13°		293°	
GWALP23-R14[d]	CG-MD /DOPC			22°	9°	249°	−44°

[a]The modified GALA analysis was based upon "model 3" of Strandberg *et al.* [31], with variable order parameter S_{ZZ}, such that $0 < S_{ZZ} < 1$. The angle $\varepsilon_{//}$ between an alanine C_α–C_β bond and the helix axis was 59.4°.[7]

[b]The rmsd, in kHz, refers to the root mean squared deviation between observed ^{2}H quadrupolar splittings and those predicted by a particular GALA fit.

[c]The values Δτ and Δρ refer to the differences in tilt and rotation, respectively, when comparing GWALP23-R14 and GWALP23 using the same method and same value of S_{ZZ}.

[d]The absolute rotation values were calculated based on the rotation angles of the backbone particles of all residues in the helix over the course of the simulation, and converted to the common reference used in the NMR calculations (the backbone particle of glycine 1). Tilt values were calculated from fitting a Gaussian distribution to the TM region of the graph.